Journal of Pharmaceutical Analysis 14 (2024) 100973

Contents lists available at ScienceDirect

Journal of Pharmaceutical Analysis

journal homepage: www.elsevier.com/locate/jpa

Original article

Pharmacometabolomics and mass spectrometry imaging approach to reveal the neurochemical mechanisms of *Polygala tenuifolia*

Qian Li [a, b], Jinpeng Bai [a, c], Yuxue Ma [a, b], Yu Sun [a, c], Wenbin Zhou [a, b], Zhaoying Wang [a, c], Zhi Zhou [a, c], Zhonghua Wang [a, c], Yanhua Chen [a, c, **], Zeper Abliz [a, b, c, d, *]

[a] Key Laboratory of Mass Spectrometry Imaging and Metabolomics (National Ethnic Affairs Commission), Minzu University of China, Beijing, 100081, China
[b] Key Laboratory of Ethnomedicine of Ministry of Education, School of Pharmacy, Minzu University of China, Beijing, 100081, China
[c] Center for Imaging and Systems Biology, College of Life and Environmental Sciences, Minzu University of China, Beijing, 100081, China
[d] State Key Laboratory of Bioactive Substance and Function of Natural Medicines, Institute of Materia Medica, Chinese Academy of Medical Sciences, Peking Union Medical College, Beijing, 100050, China

ARTICLE INFO

Article history:
Received 24 December 2023
Received in revised form
2 March 2024
Accepted 25 March 2024
Available online 28 March 2024

Keywords:
Polygala tenuifolia
Pharmaceutical metabolomics
Spatially resolved metabolome
Sedative-hypnotic
Neurochemical mechanisms

ABSTRACT

Polygala tenuifolia, commonly known as Yuanzhi (YZ) in Chinese, has been shown to possess anti-insomnia properties. However, the material basis and the mechanism underlying its sedative-hypnotic effects remain unclear. Herein, we investigated the active components and neurochemical mechanism of YZ extracts using liquid chromatography tandem mass spectrometry (LC-MS/MS)-based pharmacometabolomics and mass spectrometry imaging (MSI)-based spatial resolved metabolomics. According to the results, 17 prototypes out of 101 ingredients in the YZ extract were detected in both the plasma and brain, which might be the major components contributing to the sedative-hypnotic effects. Network pharmacology analysis revealed that these prototypes may exert their effects through neuroactive ligand-receptor interaction, serotonergic synapse, dopaminergic synapse, and dopaminergic synapse, among other pathways. LC-MS/MS-based targeted metabolomics and Western blot (WB) revealed that tryptophan-serotonin-melatonin (Trp-5-HT-Mel) and tyrosine-norepinephrine-adrenaline (Tyr-Ne-Ad) are the key regulated pathways. Dopa decarboxylase (DDC) upregulation and phenylethanolamine *N*-methyltransferase (PNMT) downregulation further confirmed these pathways. Furthermore, MSI-based spatially resolved metabolomics revealed notable alterations in 5-HT in the pineal gland (PG), and Ad in the brainstem, including the middle brain (MB), pons (PN), and hypothalamus (HY). In summary, this study illustrates the efficacy of an integrated multidimensional metabolomics approach in unraveling the sedative-hypnotic effects and neurochemical mechanisms of a Chinese herbal medicine, YZ.

1. Introduction

Insomnia can cause fatigue, reduced attention, impaired cognitive functioning, irritability, anxiety, and low mood during the day, negatively impacting individuals' quality of life [1]. It is an increasingly prevalent global disorder, largely attributed to chronic workplace stress, which significantly compromises human well-being and poses potential health risks [2]. Moreover, insomnia robustly correlated with depression, Alzheimer's disease, and other neurodegenerative conditions [3–5]. Insomnia is primarily managed with several hypnotics currently in use, including benzodiazepine receptor agonists, zolpidem, antihistamines. Antidepressants may provide short-term efficacy and are also associated with potential side effects such as next-day sedation, ataxia, and cognitive impairment [6]. Furthermore, the prolonged use of these medications could lead to adverse reactions, including addiction, as well as drug resistance and tolerance, among others [7]. Therefore, exploring medications with efficient sedative-hypnotic pharmacodynamic effects, as well as favorable prognostic outcomes and high clinical safety, is imperative.

* Corresponding author. Key Laboratory of Mass Spectrometry Imaging and Metabolomics (National Ethnic Affairs Commission), Minzu University of China, Beijing, 100081, China.
** Corresponding author. Key Laboratory of Mass Spectrometry Imaging and Metabolomics (National Ethnic Affairs Commission), Minzu University of China, Beijing, 100081, China.
E-mail addresses: zeper@muc.edu.cn (Z. Abliz), chenyanhua@muc.edu.cn (Y. Chen).

https://doi.org/10.1016/j.jpha.2024.100973

Polygalae Radix is derived from the root of Polygala species, including *Polygala tenuifolia* Willd. and *Polygala sibirica* L. [8], and was first documented in the ancient medicine book "Shen Nong Ben Cao Jing". According to research, *Polygala tenuifolia*, commonly known as Yuanzhi (YZ) in Chinese, is one of the top three individual herbs included in clinical prescriptions to promote tranquility and intelligence [9]. Recent scientific studies demonstrated the efficacy of YZ in treating insomnia, anxiety [10,11], Alzheimer's disease [12], Parkinson's disease [13], and depression [14], among other contemporary neurological disorders. Unlike chemical medications that typically comprise a single ingredient, YZ has a complex and diverse composition, impacting its scientific interpretation. According to previous research, xanthones, saponins, and oligosaccharide esters are the primary chemical components of YZ [15,16]. Furthermore, tenuifolin, the monomeric component of YZ, has been reported to exert sedative-hypnotic effects by significantly reduced the norepinephrine (Ne), elevated the gamma-amino butyric acid (GABA), and increased the acetylcholine (Ach) in different brain regions [11]. Some other YZ compounds might also exert sedative and hypnotic effects, but their neurochemical mechanism remains unclearly.

Pharmacometabolomics is a specialized branch of metabolomics focused on studying drug effects by analyzing endogenous and exogenous metabolites, including drug metabolite concentrations, to evaluate the feasibility of biomarker development and therapeutic value of drugs [17]. This approach can effectively elucidate the therapeutic potential of traditional Chinese medicine (TCM) medications, particularly by exploring diverse functional compounds, expediting the interpretation of their pharmacological functions and generally advancing the modern exploration of TCM drugs [18]. For instance, through liquid chromatography-mass spectrometry (LC-MS), pharmacometabolomics revealed that YZG-331 elicits sedative-hypnotic effects by modulating neurotransmitters (NTs) such as GABA, tryptophan (Trp), and serotonin (5-HT) [19]. Network pharmacology could also be employed to predict the action mechanisms of various chemical constituents of TCM medications. Furthermore, several studies recently explored the effective components and potential mechanisms of Chinese medicine by integrating serum pharmacochemistry and network pharmacology [20,21].

NTs are vital neuron-synthesized endogenous chemicals and serve as intercellular messengers upon the activation of specific receptors. They mainly include amino acid NTs like Trp and tyrosine (Tyr), and monoamine NTs such as 5-HT, dopamine (DA), peptides [22]. Various neurological and psychiatric conditions, including insomnia are prominently characterized by imbalances in the NT system [23]. Therefore, understanding the alterations in NTs could offer insights into the molecular mechanisms underlying drug actions. However, exploring the neurochemical mechanisms underlying drugs' sedative and hypnotic effects rely not only on changes in the content of NTs but also on their specific sites of action within the brain tissue. Based on the airflow-assisted desorption electrospray ionization-mass spectrometry imaging (AFADESI-MSI) technique, the spatially resolved metabolomics approach can elucidate the spatial changes in NTs [24], map metabolic networks [25], and describe the distinct mechanisms underlying the action of olanzapine and the potential sedative-hypnotic drug, YZG-331 [26,27]. However, unlike LC-MS, MSI has less sensitivity and cannot detect most NTs on a metabolic pathway. In this regard, a pharmacometabolomics approach integrating the respective advantages of LC-MS and MSI technologies could offer more comprehensive insights into the neurochemical mechanisms of the sedative-hypnotic effects of YZ.

Herein, we identified the components of YZ that permeate the plasma and brain tissues through high-resolution mass spectrometry (HRMS). Based on the *in vivo* composition, we employed network pharmacology techniques to predict the potential medication targets. We also developed a targeted metabolomics analysis method and a quantitative analysis method for 48 NTs and NTs-pathway-related metabolites, as well as five monomeric components of YZ, respectively. A temporal analysis of NTs and the five drug components was performed to identify differential metabolites. The corresponding molecular mechanisms were identified through the Western blot (WB) analysis results. Finally, spatial distribution and changes of NTs were detected through MSI.

2. Materials and methods

2.1. Chemicals and reagents

Polygala tenuifolia Willd. was acquired from the Beijing Tong Ren Tang Group (Beijing, China). In order to improve the extraction efficiency, YZ (500 g) was soaked in 70% ethanol (5 L) for 12 h and boiled twice for 1 h [28]. The decoction was then filtered, combined, and lyophilized into a dry powder. LC/MS grade acetonitrile, methanol, isopropanol, and formic acid (Thermo Fisher Scientific Inc., Burlington, MA, USA) were used in the experiment. Ultrapure water was purchased from Wahaha Co., Ltd. (Hangzhou, China). Ammonium acetate, ammonium formate, diethyl ether, and hydroxypropyl-β-cyclodextrin were purchased from Sinopharm Group Co., Ltd. (Beijing, China). Finally, 0.9% NaCl was acquired from Shijiazhuang No. 4 Pharmaceutical (Shijiazhuang, China). Polygalaxanthone III, tenuifolin, 3,6'-disinapoylsucrose, sibiricose A5, and sibiricose A6 were sourced from Chengdu Lemeitian Pharmaceutical Co., Ltd. (Chengdu, China). Biochemical compounds including asparagine, taurine (Tau), aspartate, glutamine, proline (Pro), glutamate, Tyr, phenylalanine (Phe), arginine, hypoxanthine (Hx), GABA, Trp, kynurenic acid, histidine (His), homovanillic acid (Hva), adenine, adenosine (Adn), kynurenine, 5-hydroxytryptophan (5-HTP), Ach, adrenaline (Ad), histamine (Hit), carnosine (Car), 5-HT, Ne, melatonin (Mel), 5-hydroxyindoleacetic acid (5-HIAA), glycine, inosine, l-dopa, indole, *N*-acetyl-5-hydroxytryptamine (*N*-ace-5-HTP), uracil, cytosine, thymine, l-valine (Val), l-alanine, l-leucine, cysteine, l-lysine (Lys), l-threonine, citrulline, l-methionine, uric acid, and l-carnitine hydrochloride (Sigma-Aldrich, St. Louis, MO, USA) were used for LC-MS analysis. Pentobarbital sodium and diazepam were acquired from the National Institute for Food and Drug Control (Beijing, China). The antibodies aralkylamine *N*-acetyltransferase (AANAT), acetylserotonin *O*-methyltransferase (ASMT), dopa decarboxylase (DDC), DA β-hydroxylase (DBH), and phenylethanolamine *N*-methyltransferase (PNMT), as well as His decarboxylase (HDC) were acquired from ABclonal Technology Co., Ltd. (Wuhan, China).

2.2. Animal experiment

Herein, five-week-old male Sprague-Dawley rats weighing 180—200 g procured from Vital River Laboratory Animal Technology Co., Ltd. (Beijing, China) were used.

Twenty-seven rats were used to assess the sedative-hypnotic efficacy of the YZ extract by two experiments. The rats were classified into three groups (YZ group, diazepam group, and control group). The YZ group, diazepam group, and the control group were orally administered with 3 g/kg YZ extract, 14 mg/kg diazepam, and 0.5% carboxymethyl cellulose-Na, respectively. For the body temperature and dystonia tests (six rats in each group), body temperature of rats was measured at 0, 30, 60, 90, 120, 240, 360, 480, and 600 min post-administration. Muscle tension of rats was assessed at 0, 30, 60, 90, and 120 min post-administration. Research has shown that diazepam has minimal effect on body temperature [29];

therefore, this experiment did not repeat the measurement of body temperature in the diazepam group. Additionally, nine rats were divided into three groups for sleep latency and extender tests: YZ group, diazepam group, and control group (three rats in each group). Sodium pentobarbital was intraperitoneally administered at a dosage of 42 mg/kg to 15 min, after administering YZ extract and carboxymethyl cellulose-Na.

For the analysis of the components of YZ entering blood and brain, three rats were orally administered with 0.5% carboxymethyl cellulose-Na, and the other six were each orally administered with 5 g/kg of YZ extract. After intragastric administration at 1 and 2 h ($n = 3$), the blood and brain tissues were acquired.

For the pharmacometabolomics and MSI analysis, rats were randomly assigned to two groups: control group ($n = 3$) and the YZ extract group ($n = 15$). YZ extract group was further divided into five time points (0.25, 0.83, 2, 4, and 8 h), with three animals for each time point. The sampling time points is set according to the preliminary experiment (Fig. S1) and references [30,31]. The YZ group rats were treated with 3 g/kg (a dosage calculated considering the human clinical dosage of 30 g/day, by following the standard guidelines for converting dosages between rats and human) of the YZ extract group via gavage. The control group rats received 0.5% carboxymethyl cellulose-Na. Subsequently, all the animals were anesthetized with diethyl ether, before collecting blood samples from the abdominal aorta and placing them in centrifuge tubes containing heparin sodium.

The blood samples were then centrifuged at 3,000 r/min for 10 min at 4 °C. Subsequently, the supernatants preserved at −80 °C, awaiting further experiments. The brains were promptly removed and snap-frozen in liquid nitrogen for subsequent LC-MS and AFAIDESI-MSI analyses. All samples were stored at −80 °C, awaiting analysis. This study was ethically approved by the Biological and Medical Ethics Committee of Minzu University of China (Approval No.: 2017−01).

2.3. Network pharmacology

A network pharmacology analysis was performed to explore potential targets and regulatory pathways of candidate compounds capable of crossing the blood-brain barrier (BBB) and being present in plasma. We detected 17 chemicals in both the rat brain and plasma and cross-referenced them in the PubChem (https://pubchem.ncbi.nlm.nih.gov) and SciFinder (https://scifinder.cas.org/scifinder) databases (please refer to Fig. S2 for the chemical structures). Targets in the SwissTargetPrediction database (https://www.swisstargetprediction.ch) were then predicted using the Canonical SMILES of the 17 chemicals. The “chemical-target” network was constructed using Cytoscape (version 3.7.2), with nodes representing the chemicals and targets and edges representing the interaction between nodes. Additionally, insomnia-related targets were compiled from the GeneCards (https://www.genecards.org), DisGeNET (https://www.disgenet.org), and DrugBank (https://www.drugbank.ca) databases. Subsequently, Venn diagrams were generated to compare the chemical targets with insomnia-related targets, followed by Gene Ontology (GO) and Kyoto Encyclopedia of Genes and Genomes (KEGG) pathway enrichment analyses of the cross-targets in the R platform (version 4.2.0).

2.4. Sample preparation and LC-MS analysis

Plasma samples were subjected to protein precipitation, and the supernatant aliquots (200 μL) were withdrawn, followed by drying in vacuum [32]. The dried samples were then reconstituted in 200 μL of water supplemented with 2% acetonitrile and vortexed at 2,000 r/min for 10 min at 4 °C. After centrifuging at 12,000 r/min for 10 min, all samples were filtered through a 96-well plate filter and transferred to a vial for LC-MS analysis.

For brain tissue processing, the vertical incision along the midline of the left and right hemispheres was sliced to obtain the largest coronal section of the right hemisphere. After sliced four consecutive sections for MSI, the adjacent 200 slices (approximately 200 mg) were reserved for later LC-MS analysis. Then they were homogenized with physiological saline and the protein was removed by using the protein precipitation method, which involved adding ten times the amount of acetonitrile to the brain homogenate and vortexing. Finally, 200 μL of the supernatant was obtained through similar steps as in plasma treatment. The quality control (QC) samples of plasma or brain tissue are composed of an equal mixture (10 μL of each) of all plasma or brain samples, respectively. All QC samples were applied for the same processing method. Both the plasma and brain tissue samples were used for quantitative analysis of the components in YZ and for targeted metabolomics studies. In addition, for the chemical composition analysis of YZ entering brain tissue, the brain tissue samples were processed using the protein precipitation method to remove proteins.

The LC-MS analysis comprised two main components. First, the prototype components of the YZ extract present in both the plasma and brain tissue were examined through ultra-high performance liquid chromatography (UHPLC) (ExionLC AC; AB SCIEX, Foster City, CA, USA) coupled with tandem HRMS (Triple TOF 6600; AB SCIEX). The detailed chromatographic and MS collection conditions are shown in Section S1.1 in the Supplementary data). Second, the multiple reaction monitoring (MRM) mode in UHPLC (ExionLC AC; AB SCIEX) was used in the analysis along with a triple quadrupole mass spectrometer (QTRAP 6500+; AB SCIEX) to quantify five monomeric components (polygalaxanthone III, tenuifolin, 3,6'-disinapoylsucrose, sibiricose A5, and sibiricose A6) present in the plasma and brain tissue of the YZ group, as well as 48 related NTs closely associated with sleep. Standard solutions of the five YZ monomers and 48 NTs and NTs-pathway-related metabolites were prepared with concentrations ranging from 1 to 2,000 ng/mL (2,000, 1,000, 500, 250, 125, 100, 62.5, 50, 25, 12.5, 10, 5, 2.5, and 1 ng/mL). Notably, different chromatographic columns and conditions were employed to quantify the drug monomers and NTs. The detailed chromatographic and MS collection conditions are shown in Sections S1.2 and S1.3 in the Supplementary data.

2.5. Sample preparation and AFADESI-MSI analysis

The brains were mounted on glass slides and sectioned into 10 μm slices using a Leica CM1860 cryostat (Leica Microsystem Ltd., Wetzlar, Germany) at −22 °C. All tissue sections were then stored at −80 °C until use and dried in a vacuum desiccator for approximately 30 min before analysis.

An AFADESI-MSI platform equipped with a Q-OT-qIT hybrid mass spectrometer (Orbitrap Fusion Lumos; Thermo Fisher Scientific Inc., San Jose, CA, USA) and a custom-built AFADESI ion source was used for MSI experiments. During the analysis, we continuously scanned the tissue surface in the *x*-direction at a constant rate of 160 μm/s, with a 200 μm vertical step in the *y*-direction. We acquired the mass spectra in a negative full MS mode in the following conditions: scan range, 100−1,000 Da; mass resolution, 120,000; automatic gain control target, 2×10^5; and maximum injection time, 70 ms. The spray voltage and capillary temperature were set at ±3.0 kV and 350 °C, respectively. The spray gas (nitrogen) pressure was maintained at 0.6 MPa, and the transporting gas flow was set to 45 L/min. The AFADESI spray solvent comprising acetonitrile/H_2O (8:2, *V/V*) was pumped at 6 μL/min. The distances from the sprayer to the tissue section surface and the tube were 0.6 and 3 mm, respectively. On the other hand, the distance from the orifice to the tube was 10 mm.

2.6. Method validation

The quantification method for five YZ monomers and 48 NTs and NTs-pathway-related metabolites have been validated. Using a weighted factor of $1/x^2$, we employed the weighted least squares to establish the relationship between the peak area ratio and the concentration. The lower quantification limit was defined as the lowest concentration level exhibiting a signal-to-noise ratio > 10. The relative standard deviation (RSD) of the QC samples were used to assess the precision.

Furthermore, the blank area of the sample slice was designated as the QC, and data were evaluated using a linear score graph to ensure the stability of the AFADESI-MSI analysis system. The samples were within 95% confidence interval (CI), and the relative deviation fell within the 2 standard deviation (SD) range (Fig. S3).

2.7. WB analysis

Three brain tissues from different control and YZ time subgroups were weighed to equal weights. The proteins were extracted by grinding the tissues with liquid nitrogen, after which the radio immunoprecipitation assay (RIPA) protein phosphatase inhibitor solution was added. The supernatants were collected as the total protein after centrifuging the mixture at 12,000 *g* for 10 min. Samples containing five times the loading buffer were then boiled at 95 °C for 10 min. The protein concentration was determined through the bicinchoninic acid (BCA) assay. Equivalent protein samples (100 μg/sample) were separated on a 10% sodium dodecyl sulfate-polyacrylamide gel electrophoresis (SDS-PAGE) gel and then transferred to polyvinylidene fluoride (PVDF) membranes (0.22 μm; Millipore, Billerica, MA, USA).

The nonspecific binding sites on the membranes were blocked with 0.5 g/L non-fat milk powder in Tris-buffered saline/Tween−20 (TBST) at room temperature (RT) for 1 h, after which the membranes were incubated overnight at 4 °C with the primary antibody. After extensive washing, the membranes were incubated for 1 h with anti-rabbit IgG secondary antibody conjugated with horseradish peroxidase (HRP) (ab6721, 1:5000; Abcam, Cambridge, UK) at RT, followed by reaction with the ECL Plus Substrate (Thermo Fisher Scientific Inc., Waltham, MA, USA). Finally, ImageJ (National Institutes of Health, Bethesda, MD, USA) was used to analyze the band intensities, with β-actin (ab6276, 1:3000; Abcam) as a loading control. The results were expressed as the gray scale values in relation to β-actin.

2.8. Processing and analysis of data

PeakView 2.2 (AB SCIEX) was used to identify the chemical constituents of YZ and components that entered the plasma and brain. The compounds were identified based on retention time, primary and secondary ion information, existing literature, and characteristic fragment ions. MultiQuant 3.0.3 was used in the quantitative analysis of the changes over time in the five individual components and 48 NTs and NTs-pathway-related metabolites before and after drug re-administration.

Following a previously established method [26], a spatially resolved metabolomics approach was employed to discover discriminatory metabolites in the brain. Subsequently, differential metabolites were imported into the custom-developed imaging software, MassImager (Chemmind Technologies, Beijing, China), for ion image reconstructions. After background subtraction, region-specific MS profiles were retrieved by matching high-spatial resolution hematoxylin and eosin (H&E) images and exported as a .txt file. Using a mass tolerance of 5 ppm, the file was imported into Markerview 1.2.1 (AB SCIEX) for peak picking, peak alignment, and isotope removal.

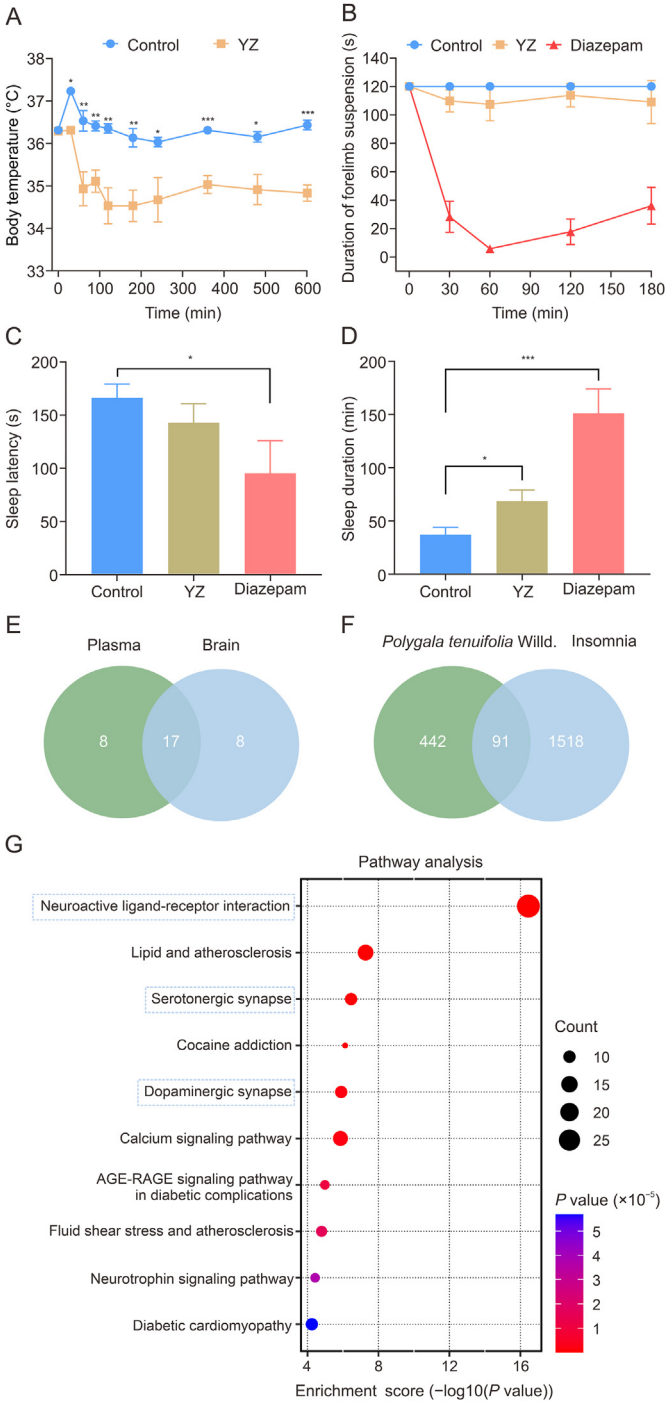

Fig. 1. Results of the sedative-hypnotic effects of *Polygala tenuifolia* (commonly known as Yuanzhi (YZ) in Chinese) and the molecular mechanism schematic diagram of network pharmacology prediction based on 17 YZ components that both enter the plasma and brain. (A–D) Evaluation results of sedative and hypnotic effects of YZ: the impact of YZ on body temperature ($n = 6$) (A), muscle tone ($n = 6$) (B), sleep latency ($n = 3$) (C), and sleep duration ($n = 3$) (D). $^{*}P < 0.05$, $^{**}P < 0.01$, and $^{***}P < 0.001$ (mean ± standard deviation (SD)). (E) Venn diagram showing the components the entered the plasma and brain. (F) Venn diagram illustrating YZ treatment targets and overall targets of insomnia diseases. (G) Kyoto Encyclopedia of Genes and Genomes (KEGG) enrichment analysis of 91 YZ treatment targets of insomnia. AGE-RAGE: advanced glycation end products-receptor for advanced glycation end.

Statistical analyses were performed using SPSS software v14.1 (Media Cybernetics, Inc., Rockville, MD, USA). Independent sample *t*-test and one-way analysis of variance (ANOVA) were used to

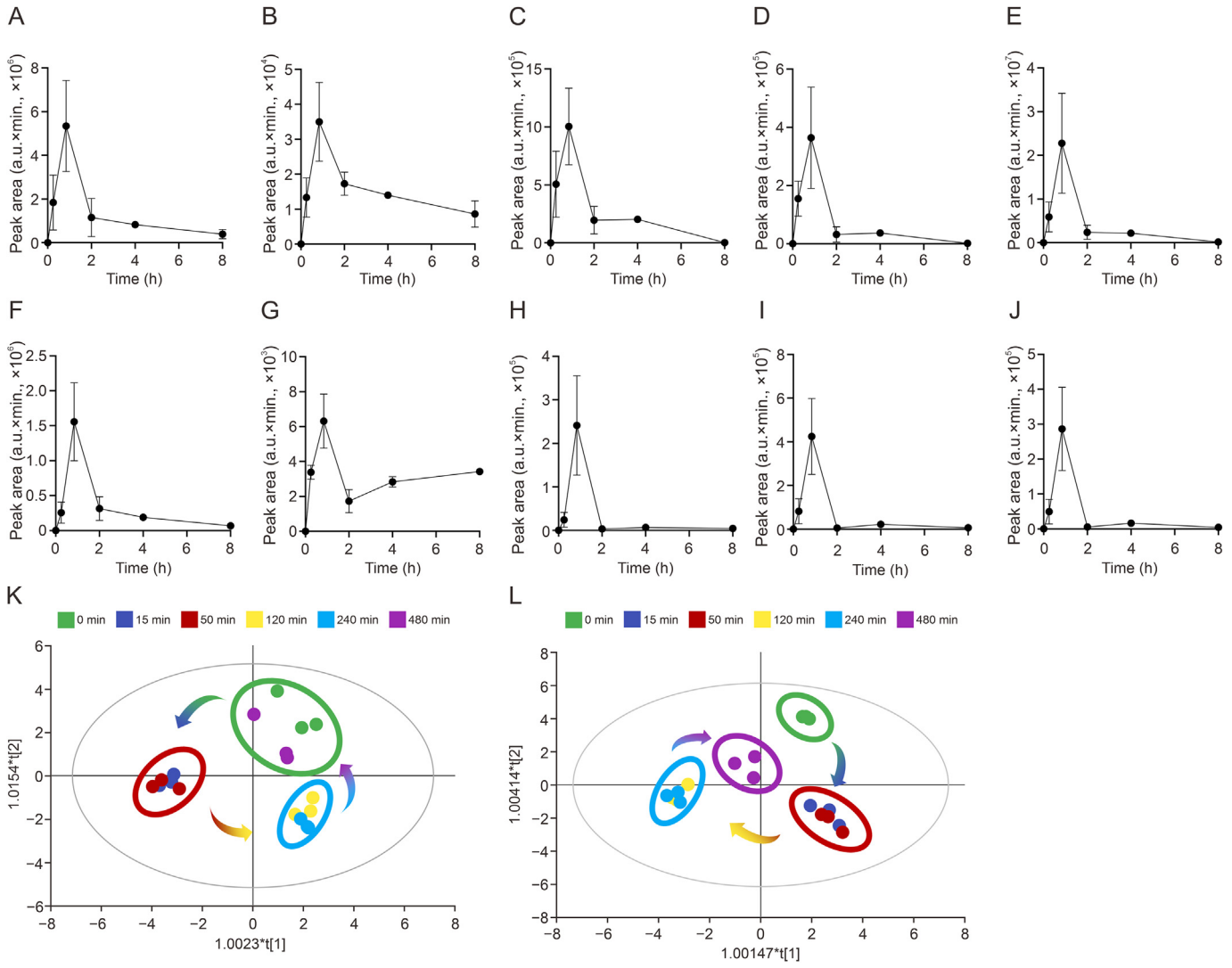

Fig. 2. The metabolism process of five *Polygala tenuifolia* (commonly known as Yuanzhi (YZ) in Chinese) representative components in plasma and brain tissue is strongly correlated with the changes of neurotransmitters (NTs) in plasma and brain tissue. (A–E) Line chart of the absorption and metabolism processes of five representative components in plasma: polygalaxanthone III (A), tenuifolin (B), 3,6'-disinapoylsucrose (C), sibiricose A5 (D), and sibiricose A6 (E). (F–J) Line chart of the absorption and metabolism processes of five representative components in brain tissue: polygalaxanthone III (F), tenuifolin (G), 3,6'-disinapoylsucrose (H), sibiricose A5 (I), and sibiricose A6 (J). (K, J) The score plots of orthogonal partial least square discriminant analysis (OPLS-DA) results are based on the plasma (K) and brain (L) NTs metabolic profiling at different time points (0, 15, 50, 120, 240, and 480 min) after administration ($n = 3$).

compare differences between two or more groups. The results were presented as mean ± SD, and those with $P < 0.05$ were considered to be statistically significant.

3. Results

3.1. The sedative and hypnotic effects of YZ

In traditional Chinese medicine, YZ has been widely used to enhance cognitive function and induce tranquility. Multiple studies have shown that YZ-derived water extracts and saponins can significantly enhance the hypnotic effect induced by pentobarbital sodium [9], by lowering sleep latency and increasing sleep duration. Herein, the 70% alcohol extract of YZ was used in the comprehensive analysis of the medicinal ingredients in YZ. Consistent with past research [33], we found that the administration of the YZ extract significantly prolonged sleep duration ($P < 0.05$). At the same time, although the body temperature was markedly decreased, it did not significantly affect sleep latency (Figs. 1A–D). The extended sleep duration implies that the orally administered 70% alcohol extracts of YZ could exert a sedative-hypnotic effect.

3.2. Serum pharmacochemistry and network pharmacology analysis of YZ

We comprehensively examined the chemical components of the 70% alcohol extracts of YZ, including organic acids, xanthones, saponins, and oligosaccharide esters [15]. Notably, 101 chemical constituents (1 carbohydrate, 4 organic acids, 23 xanthones, 36 saponins, and 37 oligosaccharide esters) were identified through ultra-performance liquid chromatography coupled with quadrupole time of flight (UPLC-Q/TOF)-MS (Fig. S4 and Table S1). Based on serum pharmacochemistry, the chemical components absorbed into the blood and target organs could be pharmacological substances [20]. Therefore, we analyzed blood and brain tissues using

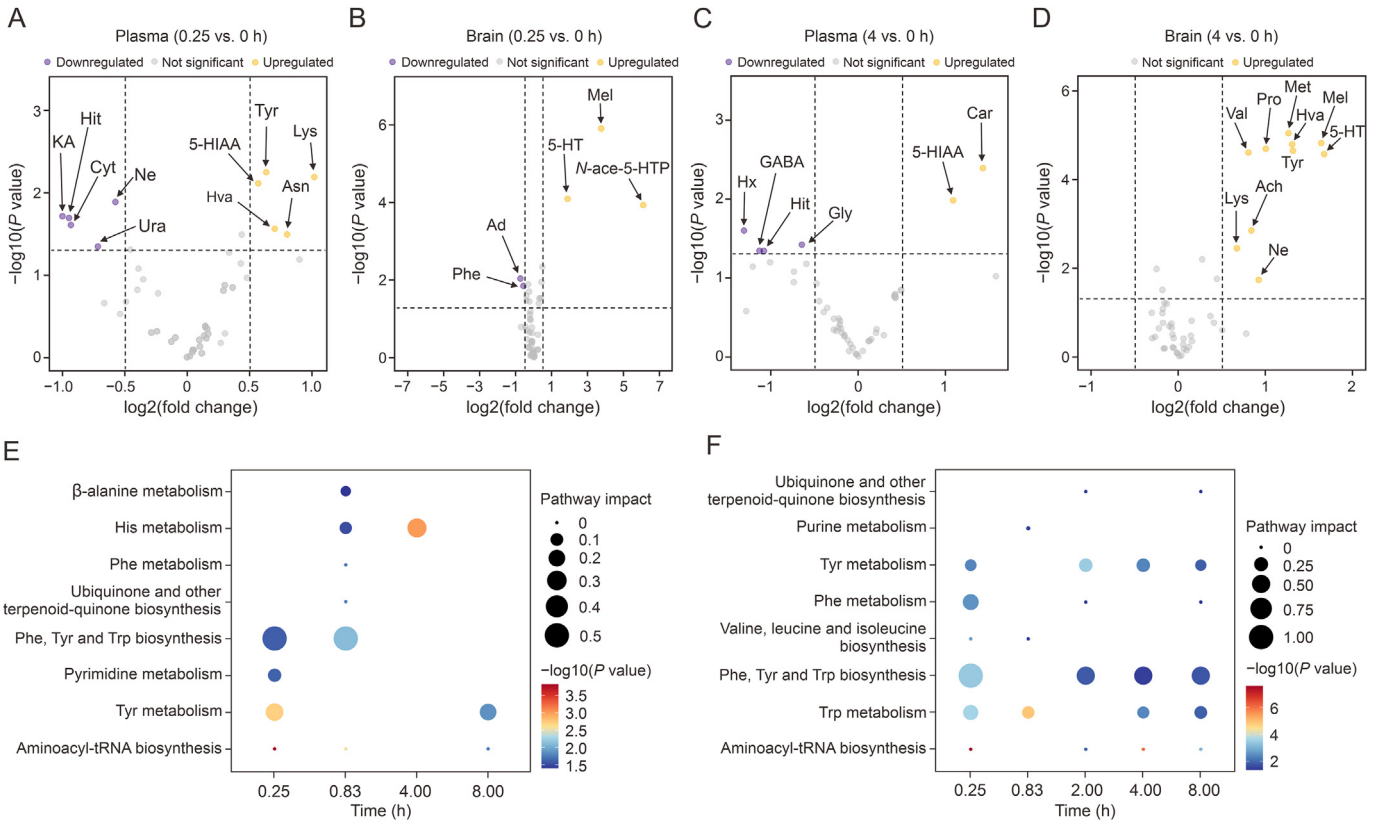

Fig. 3. Differential metabolites in plasma and brain tissue at each time point and enrichment pathway diagram of different metabolites corresponding to each time point. (A–D) Volcano maps of differential metabolites in plasma and brain tissue at 0.25 h (A, B) and 4 h (C, D) after administration ($P < 0.05$, fold change ≥ 1.4). (E, F) Figures of pathway enrichment analysis conducted by MetaboAnalyst 5.0 for plasma (E) and brain tissue (F) at different time points (0.25, 0.83, 2, 4, and 8 h vs. 0 h).KA: kynurenic acid; Hit: histamine; Cyt: cytosine; Ne: norepinephrine; Ura: uracil; Hva: homovanillic acid; 5-HIAA: 5-hydroxyindoleacetic acid; Tyr: tyrosine; Asn: asparagine; Lys: lysine; Phe: phenylalanine; Ad: adrenaline; 5-HT: serotonin; Mel: melatonin; *N*-ace-5-HTP: *N*-acetyl-5-hydroxytryptamine; Hx: hypoxanthine; GABA: gamma-amino butyric acid; Gly: glycine; Car: carnosine; Ach: acetylcholine; Val: valine; Pro: proline; Met: methionine; His: histidine; Trp: tryptophan; tRNA: transfer RNA.

LC-MS. The findings revealed 25 prototype ingredients each in the plasma (Table S2) and brain (Table S3). Among them, 17 prototype ingredients (including 2 xanthones, 6 saponins, and 9 oligosaccharide esters) entered both the plasma and the brain (Figs. 1E and S5). Fig. S6 details the identification processes by four standard references. Therefore, we hypothesized that xanthones, saponins, and oligosaccharide esters could be the active components of YZ contributing to the sedative-hypnotic effects. Hitherto, only the saponin component tenuifolin (one of the 17 prototype ingredients detected in both the plasma and the brain) has been reported to exert significant sedative-hypnotic effects [11]. On the other hand, the sedative-hypnotic effects of xanthones and oligosaccharide esters and their relevant mechanisms of action remain unclear.

We further explored the mechanism of YZ through network pharmacological analysis. First, 1,609 insomnia-related target genes were screened using the GeneCard, DisGeNET, DRUGBANK, and Online Mendelian Inheritance in Man (OMIM) databases. We found that 91 of the 533 pharmacodynamic targets of the 17 prototype ingredients detected in both the plasma and brain were associated with the target genes for insomnia (Figs. 1F and S7). Subsequently, the public target genes were subjected to the KEGG pathway enrichment analysis, and the top pathways with the smallest *P*-values were highlighted (Fig. 1G). Specifically, the analysis revealed that YZ extracts had the most significant impact on neuroactive ligand-receptor interaction, serotonergic synapse, and dopaminergic synapse, among other pathways. Consequently, we hypothesized that the 17 compounds in YZ extracts (including xanthones, saponins, and oligosaccharide esters) might exert sedative-hypnotic effects by regulating NTs.

3.3. Time-resolved regulation of plasma and brain NTs by YZ extracts utilizing a targeted metabolomics method

To elucidate the YZ mechanism *in vivo*, we developed a quantitative method for analyzing the five representative monomeric components in YZ extracts: polygalaxanthone III, tenuifolin, 3,6'-disinapoylsucrose, sibiricose A5, and sibiricose A6 (Fig. S8). Table S4 details the optimization of MS conditions, including declustering potential and collision energy. The exposure levels of these five monomeric components in YZ in plasma and brain were analyzed at different time points, revealing that all five monomeric components peaked at 0.83 h in both plasma and brain (Figs. 2A–J). Furthermore, tenuifolin demonstrated significant reabsorption in the brain at 2–4 h (Fig. 2G).

An LC-MS/MS-based targeted metabolomics approach related to NTs was used to further investigate the hypothesis that YZ might exert sedative-hypnotic effects by modulating NTs [19]. Herein, 46 (excluding DA and tyramine) and 48 NTs and NTs-pathway-related metabolites were detected in the blood and brain homogenates, respectively (Fig. S9). Table S5 details the MS conditions for these NTs. Quantitative method validation procedures, including linearity, were also conducted. Tables S6 and S7 show the regression equations, correlation coefficients, dynamic ranges and precision. The results indicate that the two methods

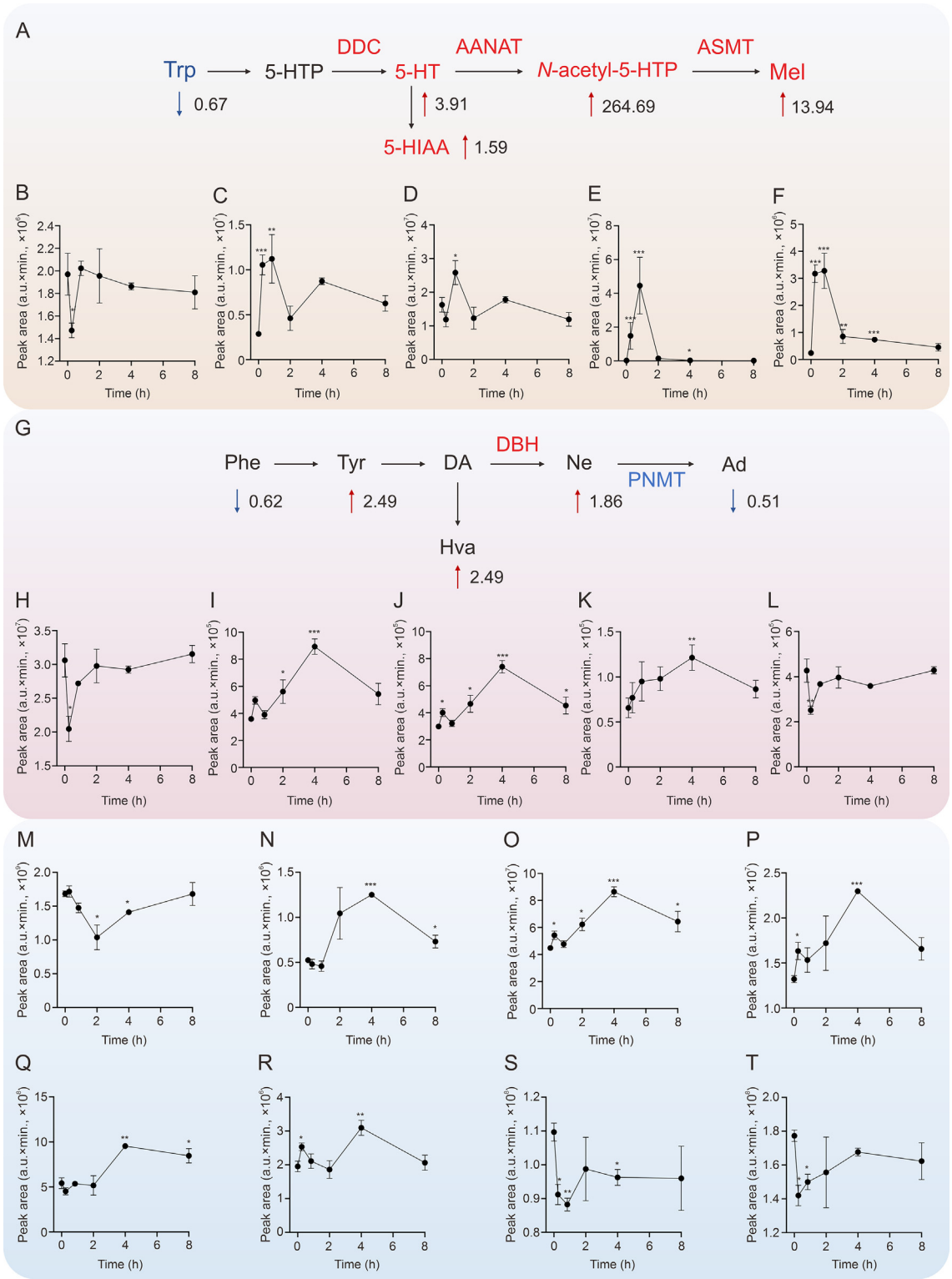

Fig. 4. Alterations in differential metabolites over time in brain after administration of the *Polygala tenuifolia* (commonly known as Yuanzhi (YZ) in Chinese) extract. (A–F) Line charts of differential metabolites in the tryptophan-serotonin-melatonin (Trp-5-HT-Mel) metabolic pathway (A), including Trp (B), 5-HT (C), 5-hydroxyindoleacetic acid (5-HIAA) (D), *N*-acetyl-5-hydroxytryptamine (*N*-ace-5-HTP) (E), and Mel (F). (G–L) Line charts of differential metabolites in the tyrosine-norepinephrine-adrenaline (Tyr-Ne-Ad) metabolism pathway (G), including phenylalanine (Phe) (H), Tyr (I), homovanillic acid (Hva) (J), Ne (K), and Ad (L). (M–T) Line charts of some other important differential neurotransmitters, such as adenosine (Adn) (M), methionine (N), proline (Pro) (O), valine (Val) (P), acetylcholine (Ach) (Q), lysine (Lys) (R), serine (S), and threonine (T) also undergo significant changes over time. The line chart illustrating significant changes in other neurotransmitter (NTs) over time. Red arrow ↑: the largest upregulated fold compared with pre-administration; blue arrow ↓: the largest downregulated fold; the change significance of *t*-test, $^{*}P < 0.05$, $^{**}P < 0.01$, and $^{***}P < 0.001$ (mean ± standard deviation (SD)), compared with 0 min at different time points. DDC: dopa decarboxylase; AANAT: aralkylamine *N*-acetyltransferase; ASMT: acetylserotonin *O*-methyltransferase; DBH: dopamine (DA) β-hydroxylase; PNMT: phenylethanolamine *N*-methyltransferase.

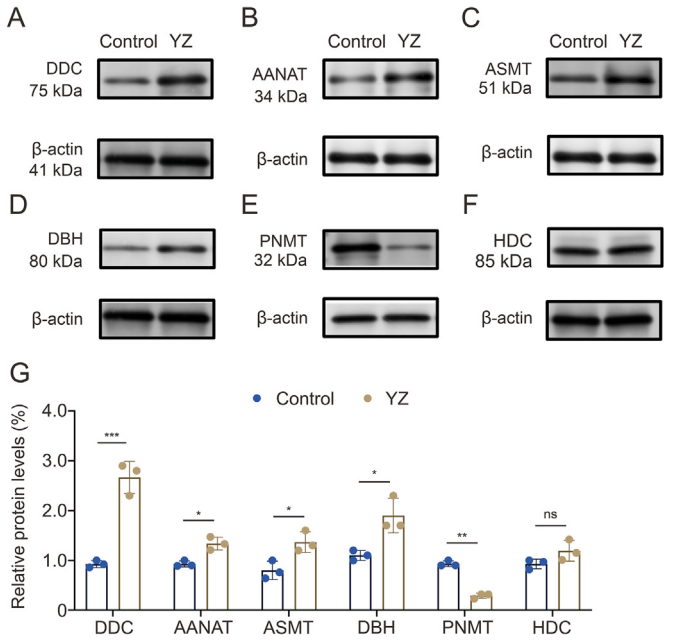

Fig. 5. Results of Western blot (WB) analysis of neurotransmitter-regulating proteins closely associated with sleep. (A–F) The expression levels of dopa decarboxylase (DDC) (A), aralkylamine *N*-acetyltransferase (AANAT) (B), acetylserotonin *O*-methyltransferase (ASMT) (C), dopamine (DA) β-hydroxylase (DBH) (D), phenylethanolamine *N*-methyltransferase (PNMT) (E), and histidine (His) decarboxylase (HDC) (F) as determined by WB. (G) The scatter bar chart of the statistical results of various proteins. $^{*}P < 0.05$, $^{**}P < 0.01$, and $^{***}P < 0.001$ (mean ± standard deviation (SD)). ns: not significant. YZ: *Polygala tenuifolia* (commonly known as Yuanzhi (YZ) in Chinese).

presented satisfied linearity and RSD, and could be applied in investigating the 48 NTs and NTs-pathway-related metabolites in the blood and brain.

The orthogonal partial least square discriminant analysis (OPLS-DA) was used in the targeted metabolomic study of plasma and brain homogenates at various time points. The OPLS-DA score plots showed that the plasma and brain homogenate samples at 15 and 0.83 h after administration as well as at 2 and 4 h clustered together, whereas they showed a tendency to return to the pre-administration levels at 8 h (Figs. 2K and L). Their change patterns were consistent with those of active ingredients in YZ extracts. This implies that YZ exerts a time-dependent effect on NTs in plasma and brain, gradually returning to the pre-administration state after 8 h. The significantly disrupted metabolites ($P < 0.05$, fold change ≥ 1.4) post-treatment with YZ at various time points are shown in volcano plots (Figs. 3A–D and S10) and Tables S8 (plasma) and S9 (brain). It is evident that compared to the plasma, YZ regulates NTs in the brain more prominently (Figs. 3E and F). In addition to the significant regulation of His metabolism in plasma alone, Tyr metabolism, Trp metabolism, as well as Phe, Tyr, and Trp biosynthesis are all significantly regulated in both the plasma and brain. Therefore, we subsequently thoroughly explored alterations in NT in the brain (including His) to better clarify and offer more insights into this study's primary findings.

In-depth analysis of Trp metabolism and biosynthesis revealed a significant decrease in Trp and a considerable increase in 5-HT, *N*-ace-5-HTP, and Mel (Figs. 4A–F). Notably, Mel increased more than ten times within 0.25 and 0.83 h post-treatment with YZ. However, the Mel levels decreased dramatically after 2 h. Mel's dynamic change over time is almost consistent with that of the active ingredients in YZ. Coincidentally, Mel is an endogenous sedative-hypnotic metabolite closely related to sleep. Simultaneously, after 0.83 h of treatment, its precursor *N*-ace-5-HTP was upregulated by as much as 265 times. Furthermore, there was a 3.9-fold increase in 5-HT levels after 0.83 h of treatment. Therefore, the YZ extract may induce sedative-hypnotic effects by modulating the Trp-5-HT-Mel metabolic pathway.

Regarding the metabolism and biosynthesis of Phe and Tyr, we discovered that Phe was notably downregulated by 1.6 times at 0.25 h (Figs. 4G and H), whereas Tyr was significantly upregulated by 2.5 times at 4 h (Fig. 4I), with Hva also significantly upregulated by 2.5 times at 4 h (Fig. 4J). Moreover, Ne was significantly upregulated by 1.9 times at 4 h (Fig. 4K), whereas Ad was notably downregulated by 2 times at 0.25 h (Fig. 4L). Central Ne regulates body temperature, sleep and arousal, mental and emotional activity, and cardiovascular activity, whereas Ad primarily regulates cardiovascular activity [34,35]. Herein, Ne was significantly upregulated in the brain tissue homogenate, demonstrating that YZ could regulate Ad and Ne. This finding was further verified by WB molecular experiments, which revealed significant upregulation and downregulation of DBH (the Ne metabolizing enzyme) and the Ad metabolizing enzyme PNMT, respectively. Therefore, the YZ extract could also induce sedative-hypnotic effects by regulating Ad in the Tyr-Ne-Ad pathway.

Furthermore, there are some other NT-related metabolites associated with sleep that showed regular change patterns post-treatment (Figs. 4M–T). Adn, a prominent physiological mediator of sleep homeostasis, decreased at 0.83 h, becoming statistically significantly different at 2 and 4 h, but recovered after 8 h (Fig. 4M). This pattern is consistent with the hypothesis that Adn promotes sleep during wakefulness, and decreases during sleep [36,37]. Additionally, Ach, which promotes both sleep and arousal in mammals [38], increased significantly at 4 and 8 h (Fig. 4Q). Cholinergic neurons in various brain regions have been reported to promote wakefulness, as well as rapid eyes movement (REM) or non-rapid eye movement (NREM) sleep [39,40].

Notably, Hit levels in plasma decreased significantly after 15 and 240 min (Fig. S11), implying that the YZ extract could directly regulate Hit levels. Hit is an awakening drug, and the administration of Hit or H1 receptor agonists induces wakefulness, whereas the administration of H1 receptor antagonists promotes sleep [41]. Therefore, Hit downregulation in plasma at 15 min implies that YZ may exert sedative-hypnotic effects by inhibiting Hit.

Overall, NT research indicates that YZ may induce sedative-hypnotic effects by modulating the Trp-5-HT-Mel and Tyr-Ne-Ad pathways, as well as Ad, Ach, and Hit metabolism. The related metabolic enzymes were further validated by WB. DDC (Fig. 5A), AANAT (Fig. 5B), and ASMT (Fig. 5C) expression increased significantly, especially for DDC, potentially explaining the changes over the Trp-5-HT-Mel pathway. Meanwhile, it revealed a significant upregulation and downregulation of DBH (Fig. 5D) and PNMT (Fig. 5E), respectively, potentially accounting for alterations in the associated metabolites in the Tyr-Ne-Ad metabolic pathway. On the other hand, the WB results of brain tissue showed that the Hit regulatory protein, HDC (Fig. 5F), was not significantly regulated. The statistical data of the WB experiment are shown in Fig. 5G and Table S10.

3.4. Precisely mapping spatial fluctuations in brain NTs through spatially resolved metabolomics

Herein, targeted metabolomics elucidated two crucial pathways: Trp-5-HT-Mel and Tyr-Ne-Ad. However, this outcome lacks the spatial distribution information. According to research, NTs have distinct distributions in the brain, with diverse functional roles [42]. Since NTs have a distinctive distribution, an accurate

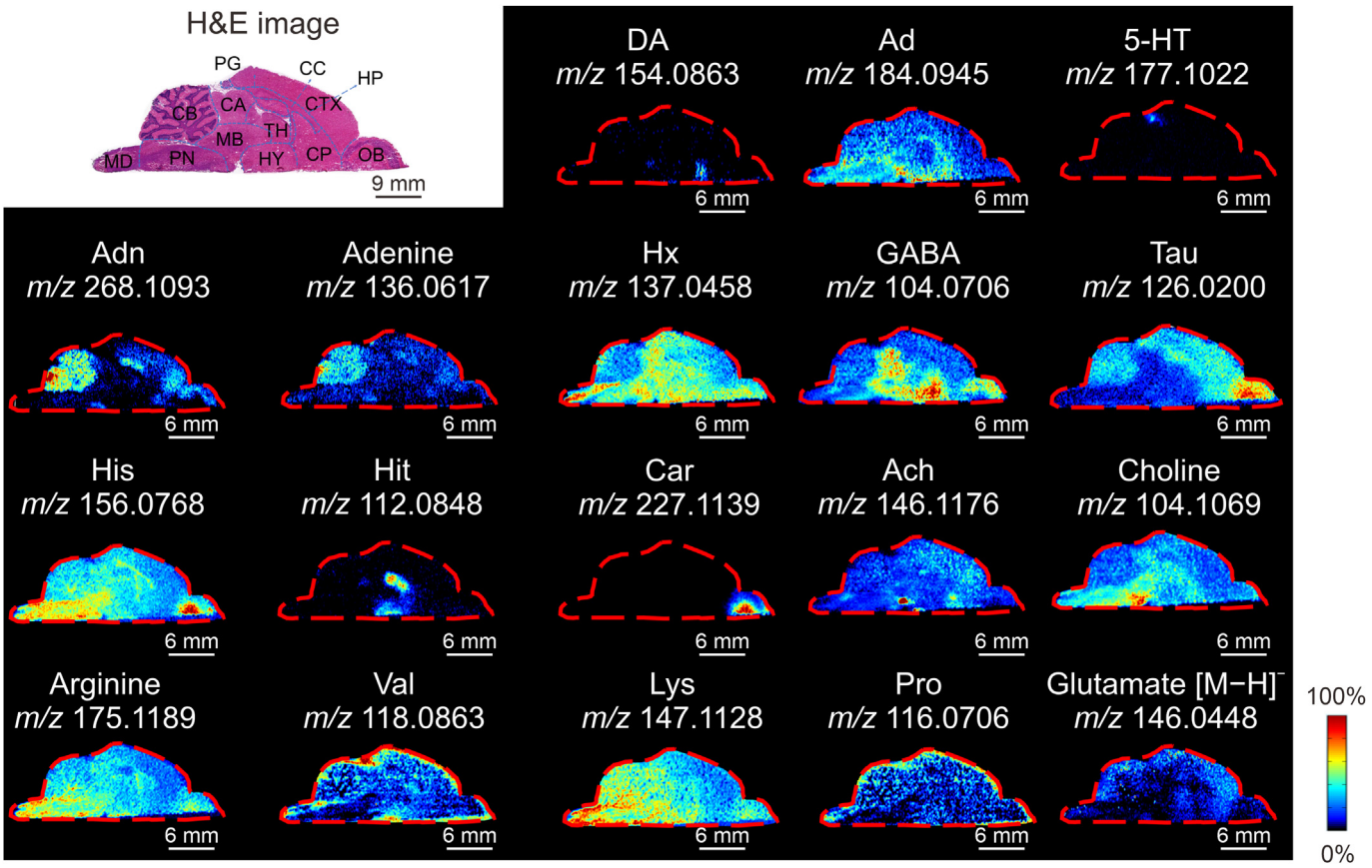

Fig. 6. The distribution map of neurotransmitters (NTs) in various brain regions. H&E: hematoxylin and eosin; PG: pineal gland; CC: corpus callosum; HP: hippocampus; CB: cerebellar; CA: cerebral aqueduct; CTX: cerebral cortex; MB: middle brain; TH: thalamus; MD: medulla; PN: pons; HY: hypothalamus; CP: caudate putamen; OB: olfactory bulb; DA: dopamine; Ad: adrenaline; 5-HT: serotonin; Adn: adenosine; Hx: hypoxanthine; GABA: gamma-amino butyric acid; Tau: taurine; His: histidine; Hit: histamine; Car: carnosine; Ach: acetylcholine; Val: valine; Lys: lysine; Pro: proline.

interpretation of their spatial alteration could offer more comprehensive insights into the sedative-hypnotic mechanisms of YZ. Herein, an AFADESI-MSI-based spatially resolved metabolomics method was employed [25]. According to the results, different NTs exhibited different spatial distributions in the brain, including the specific 5-HT distributions in the pineal gland (PG), DA in the caudate putamen (CP) [43], Adn in the cerebellar (CB) and cerebral cortex (CTX), Hit in the thalamus (TH) and hypothalamus (HY) [27], and Car in the olfactory bulb (OB). Notably, some NTs, including GABA, Tau, and His, among others, were distributed throughout the brain. However, GABA was concentrated in the HY and cerebral aqueduct (CA), Tau was concentrated in the OB, CTX, and CB [26], and His was concentrated in the OB, pons (PN), and corpus callosum (CC) [25] (Fig. 6). Since the distinctive distribution of NTs was consistent with that in previous studies, it could be used to examine the spatial changes of NTs in the brain before and after treatment.

Consistent with the LC-MS findings, the imaging results revealed a notable increase in 5-HT expression in the PG (Figs. 7A and B and Table S11). However, its precursor 5-HTP and product metabolites *N*-ace-5-HTP and Mel were not detected, potentially due to the lower sensitivity of MSI compared to that of LC-MS. It has been established that Mel is primarily synthesized in the PG, where it exerts sedative-hypnotic effects [44]. Therefore, based on the findings of LC-MS and WB molecular experiments, it is highly likely that the YZ extract could exert sedative-hypnotic effects by activating the metabolic enzymes of DDC, AANAT, and ASMT of the Trp-5-HT-Mel pathway in the PG.

In addition, imaging results revealed a significant decrease in DA in the striatum, but LC-MS results found no significant change in DA, which may be due to the disruption of DA by tissue homogenization in the striatum. DA neuron system mainly originates in the substantia nigra pars compacta and terminates in the CP [45]. This suggests that YZ may exert its effect by decreasing DA levels in the CP (Fig. 7C). Consistent with LC-MS results, we also observed a significant decrease in Ad throughout the brain, particularly in the PN, middle brain (MB), HY, and TH. (Fig. 7D). Based on LC-MS and WB results, we speculate that the YZ extract exerts sedative and hypnotic effects by decreasing the PNMT metabolic enzymes of the Tyr-Ne-Ad metabolic pathway in regions such as PN, MB, HY, and TH.

Moreover, in concordance with LC-MS results, Adn showed a significant decline in the CB and CTX regions (Fig. 7E). Although His and Hit did not exhibit significant alterations in brain homogenate overall, their distinct regional patterns are noteworthy. Specifically, His showed significant downregulation in the HY, CC, and CB brain regions (Fig. 7F), while Hit displayed significant downregulation in TH (Fig. 7G). This is consistent with the feature that the histaminergic system exists in the HY and projects to other brain regions [41]. LC-MS-based metabolomics results showed a downward trend in Hit levels in brain tissue, with a significant decrease in Hit in TH among the MSI results and a significant decrease in Hit in plasma. Altogether, these results provide evidence that YZ might influence the Hit pathway.

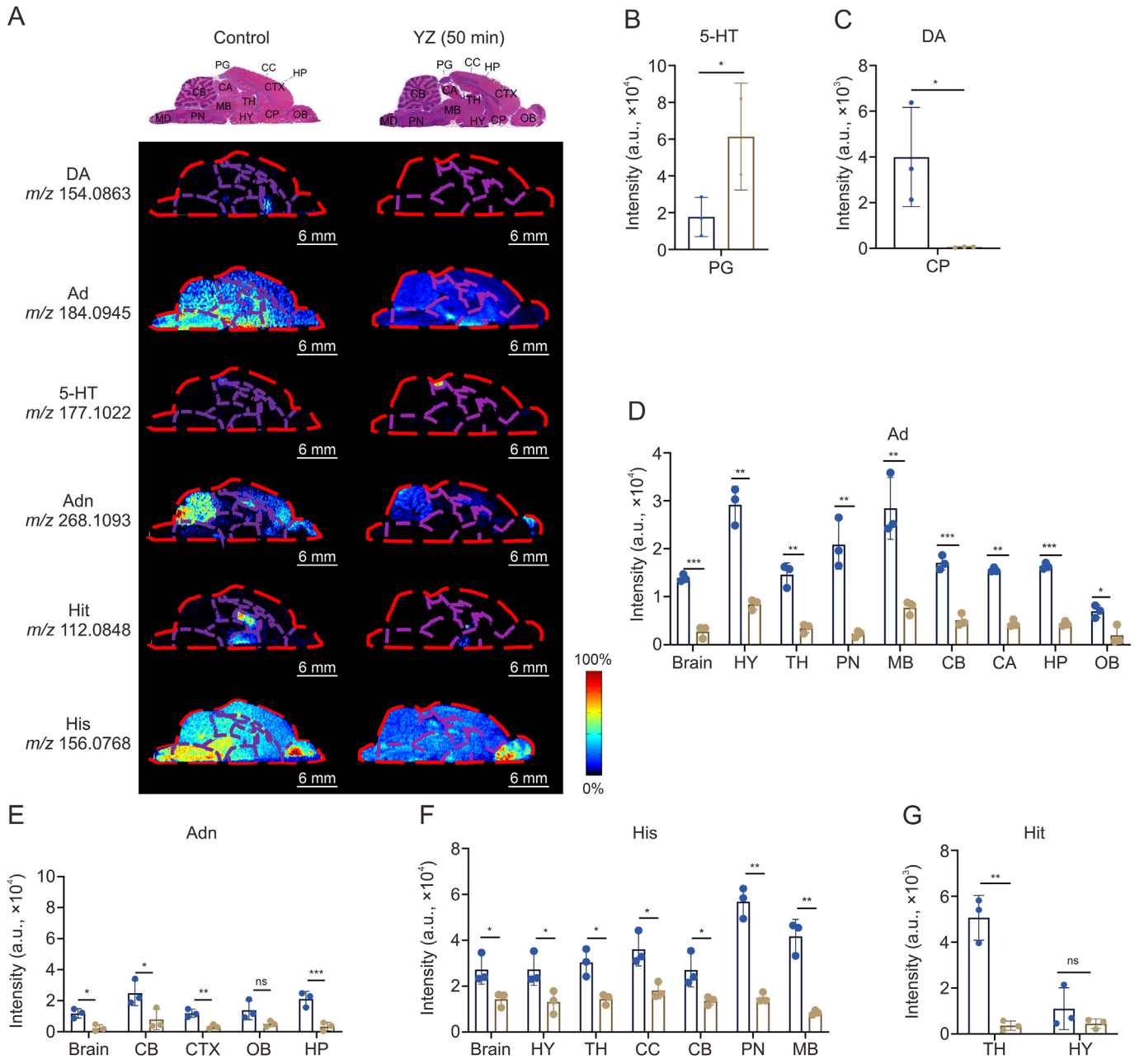

Fig. 7. Targeted imaging analysis of key differential metabolites based on liquid chromatography tandem mass spectrometry (LC-MS/MS) screening with the mass spectrometry imaging (MSI). (A) Images of neurotransmitters (NTs) with significant differences ($n = 3$). (B–G) Scatter bar charts of spatial distribution differences of serotonin (5-HT) (B), dopamine (DA) (C), adrenaline (Ad) (D), adenosine (Adn) (E), histidine (His) (F), and histamine (Hit) (G) in different brain regions. The scatter bar charts in blue represents the control group, while the one in brown represents the group treated with YZ. $^{*}P < 0.05$, $^{**}P < 0.01$, and $^{***}P < 0.001$ (mean ± standard deviation (SD)). ns: not significant. H&E: hematoxylin and eosin; PG: pineal gland; CB: cerebellar; CA: cerebral aqueduct; CC: corpus callosum; CTX: cerebral cortex; HP: hippocampus; MD: medulla; PN: pons; MB: middle brain; TH: thalamus; HY: hypothalamus; CP: caudate putamen; OB: olfactory bulb.

4. Discussion

By integrating LC-MS targeted metabolomics and spatially resolved metabolomics to investigate the sedative and hypnotic components of YZ and their underlying molecular mechanisms, we identified xanthones, saponins, and oligosaccharide esters as potential active components. These constituents may exert a sedative-hypnotic effect by modulating NTs. With the results of the time-resolved analysis of NTs and their related metabolites in plasma and brain homogenate, as well as their spatial changes and the expression of corresponding metabolic enzymes, we found that the YZ extract may primarily activate the metabolic enzymes DDC, AANAT, and ASMT of Trp-5-HT-Mel pathway in the PG to increase 5-HT, *N*-acetyl-5-HTP, and Mel. At the same time, it may inhibit PNMT of Tyr-Ne-Ad pathway mainly in PN, MB, HY, and TH to decrease Ad, activate DBH to increase Ne, and downregulate DA in the CP. Moreover, Adn, the well-known physiological mediator of sleep homeostasis, was significantly reduced in CB and CTX. Similarly, Hit decreased significantly in TH. These changes in NT after administration may explain the sedative and hypnotic effects of YZ extract.

Currently, most studies on the effects of sedative and hypnotic drugs on NTs have utilized enzyme-linked immunosorbent assay

(ELISA) [46,47] and LC-MS [48]. However, the ELISA method cannot detect numerous NTs simultaneously. In addition, many studies have utilized LC-MS to detect changes in NTs before and after administration, but they do not show spatial changes in NTs to allow researchers explain the mechanism of drugs. The spatial-resolved metabolomics has enabled researchers to study the target and mechanism of the sedative hypnotic candidate drug YZG-331 [26,27]. In this study, we propose an integrated metabolomics approach based on LC-MS and AFADESI-MSI-based metabolomics to provide highly sensitive analysis of NTs and simultaneously characterize their time and spatial-resolved changes after administration. The findings indicate complementarity between the two methods. LC-MS targeted analysis allows for a highly sensitive assessment of 48 NTs and NTs-pathway-related metabolites in both plasma and brain homogenate. When integrated with the *in vivo* metabolic processes of representative ingredients and the time-dependent changes in NTs following administration, it becomes feasible to infer the modulated metabolic pathways. The spatially resolved metabolomics may supplement the spatial distribution characteristics of metabolites, improve the prediction of regulated regions, and further confirm the molecular mechanism of drug sedative-hypnotic effects based on the correlation between this region and sedative hypnosis.

Currently, the commonly used sedative and hypnotic drugs are benzodiazepines. They exert their actions on the central nervous system (CNS) by affecting the GABAergic transmission [49], stimulating Mel receptors [50], and inhibiting the wake promoting effects of Hit via H1 receptor antagonism [51]. In addition, 5-HT reuptake inhibitors and Ne reuptake inhibitors have been applied as antidepressants which also possess certain sedative and hypnotic effects [52]. All these drugs can regulate of NTs. However, they can easily cause resistance and addiction to sedative and hypnotic drugs [53]. YZ, as a traditional sedative and hypnotic Chinese medicine, is non-toxic and can be used for a long time [54]. Findings from recent studies indicate that YZ can increase the content of 5-HT and GABA [33]. In this study, we found that YZ extract exerted pharmacological effects via multiple *in vivo* components, and its effects have multi-target characteristics. It may potentially activate the metabolic enzymes DDC, AANAT, and ASMT within the Trp-5-HT-Mel pathway in the PG, leading to sedative and hypnotic effects. Moreover, the PNMT metabolic enzymes in the Tyr-Ne-Ad metabolic pathway might experience downregulation in regions such as PN, MB, HY, and TH. These enzymes serve as key targets for addressing depression. Sleep disorders have been reported in many depressed patients [55]. Notably, 60%–80% of patients with major depressive disorder present with symptoms of insomnia [56]. Furthermore, Adn was significantly decreased in the CB and CTX regions. The substantial alterations in Hit in TH and the decreasing trend observed in brain homogenate promoted us to postulate that YZ may regulate Hit pathway in TH (Fig. 8).

However, due to the sensitivity limitations of MSI, the precise localization of *N*-acetyl-5-HTP, Mel, and Ne in brain tissue was not detected. Obtaining insights into alterations in those crucial metabolites within the brain would further elucidate the mechanism of YZ. In future, researchers should explore *in situ* derivatization techniques to enhance the sensitivity of detecting these relevant NTs. Furthermore, the different dosages of YZ extract would be explored. And the enzyme Trp 5-monooxygenase (Trp hydroxylase 1 and 2) involved in the conversion of Trp to 5-HTP is also worth further investigation.

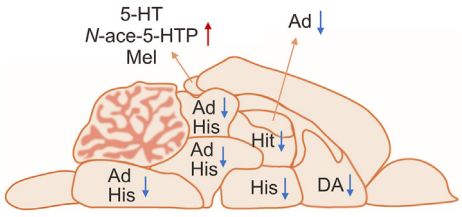

Fig. 8. Possible molecular mechanisms diagram of the sedative and hypnotic effects of extracts from *Polygala tenuifolia* (commonly known as Yuanzhi (YZ) in Chinese). 5-HT: serotonin; *N*-ace-5-HTTP: *N*-acetyl-5-hydroxytryptamine; Mel: melatonin; Ad: adrenaline; His: histidine; Hit: histamine; DA: dopamine.

5. Conclusion

By investigating the sedative and hypnotic effects of the YZ extract, we comprehensively analyzed its chemical components and penetration into the plasma and brain tissues. In addition, we determined the potential pharmacological basis through which YZ exerts sedative and hypnotic effects. Through the application of network pharmacology, time-resolved targeted metabolomics, spatially resolved metabolomics, and WB molecular experiments, we showed that YZ exerts sedative and hypnotic effects via the Trp-5-HT-Mel and Tyr-Ne-Ad metabolic pathways. In addition, based on AFADESI-MSI, we speculated the regions of action in the brain. Our results suggest that the combined use of LC-MS and MSI techniques not only determines differential information of key metabolites but also provide spatial distribution information, which allows researchers to explore the mechanism of sedative and hypnotic drugs.

CRediT author statement

Qian Li: Methodology, Data curation, Investigation, Writing - Original draft preparation; **Jinpeng Bai:** Data curation, Visualization; **Yuxue Ma** and **Yu Sun:** Methodology, Investigation; **Wenbin Zhou** and **Zhaoying Wang:** Resources, Formal analysis; **Zhi Zhou** and **Zhonghua Wang:** Formal analysis; **Yanhua Chen:** Conceptualization, Supervision, Writing - Reviewing and Editing, Funding acquisition; **Zeper Abliz:** Conceptualization, Supervision, Writing - Reviewing and Editing, Funding acquisition.

Declaration of competing interest

The authors declare that there are no conflicts of interest.

Acknowledgments

The authors thank the financial support from the National Key R&D Program of China (Grant No: 2022YFC3401003), the National Natural Science Foundation of China (Grant No: 21927808), the National Natural Science Foundation of China (Grant No: 22104160), the National Key Research and Development Program of China (Grant No: 2017YFC1704006), and the Innovation Team of Ethnomedicine of National Ethnic Affairs Commission, China. We thank all the research staff who contributed to the study.

The authors would like to thank MJEditor (www.mjeditor.com) for its linguistic assistance during the preparation of this manuscript.

Appendix A. Supplementary data

Supplementary data to this article can be found online at https://doi.org/10.1016/j.jpha.2024.100973.

References

[1] D. Riemann, F. Benz, R.J. Dressle, et al., Insomnia disorder: State of the science and challenges for the future, J. Sleep Res. 31 (2022), e13604.

[2] X. Huang, H. Jiang, J. Pei, et al., Study on the potential mechanism, therapeutic drugs and prescriptions of insomnia based on bioinformatics and molecular docking, Comput. Biol. Med. 149 (2022), 106001.
[3] I. Bjorøy, V.A. Jørgensen, S. Pallesen, et al., The prevalence of insomnia subtypes in relation to demographic characteristics, anxiety, depression, alcohol consumption and use of hypnotics, Front. Psychol. 11 (2020), 527.
[4] D.J. Buysse, J. Angst, A. Gamma, et al., Prevalence, course, and comorbidity of insomnia and depression in young adults, Sleep 31 (2008) 473–480.
[5] L. Zhang, L. Cheng, T. Wang, et al., Chain mediating effect of insomnia, depression, and anxiety on the relationship between nightmares and cognitive deficits in adolescents, J. Affect. Disord. 322 (2023) 2–8.
[6] K.A. Wafford, B. Ebert, Emerging anti-insomnia drugs: Tackling sleeplessness and the quality of wake time, Nat. Rev. Drug Discov. 7 (2008) 530–540.
[7] A.N. Edinoff, N. Wu, Y.T. Ghaffar, et al., Zolpidem: Efficacy and side effects for insomnia, Health Psychol. Res. 9 (2021), 24927.
[8] C.P. Commission, Pharmacopoeia of the Peoples Republic of China, China Medical Science Press, Beijing, 2020, pp. 163–166.
[9] L. Zhang, Y. Yong, L. Deng, et al., Therapeutic potential of *Polygala* saponins in neurological diseases, Phytomedicine 108 (2023), 154483.
[10] Y. Yao, M. Jia, J. Wu, et al., Anxiolytic and sedative-hypnotic activities of polygalasaponins from *Polygala tenuifolia* in mice, Pharm. Biol. 48 (2010) 801–807.
[11] Q. Cao, Y. Jiang, S. Cui, et al., Tenuifolin, a saponin derived from *Radix* Polygalae, exhibits sleep-enhancing effects in mice, Phytomedicine 23 (2016) 1797–1805.
[12] R. Jesky, H. Chen, The neuritogenic and neuroprotective potential of senegenin against Aβ-induced neurotoxicity in PC 12 cells, BMC Complement. Altern. Med. 16 (2016), 26.
[13] M.A. Lacaille-Dubois, C. Delaude, A.C. Mitaine-Offer, A review on the phytopharmacological studies of the genus *Polygala*, J. Ethnopharmacol. 249 (2020), 112417.
[14] Z. Jin, N. Gao, J. Zhang, et al., The discovery of Yuanzhi-1, a triterpenoid saponin derived from the traditional Chinese medicine, has antidepressant-like activity, Prog. Neuropsychopharmacol. Biol. Psychiatry 53 (2014) 9–14.
[15] T. Li, Z. Zhou, K. Zhang, et al., Direct infusion-tandem mass spectrometry combining with data mining strategies enables rapid chemome characterization of medicinal plants: A case study of *Polygala tenuifolia*, J. Pharm. Biomed. Anal. 204 (2021), 114281.
[16] L. Liu, W.-H. Feng, X.-Q. Liu, et al., Research progress on Polygalae *Radix*, Zhongguo Zhong Yao Za Zhi 46 (2021) 5744–5759.
[17] S. Grover, K.S. Kasudhan, N. Murali, et al., Pharmacometabolomics-guided clozapine therapy in treatment resistant schizophrenia: Preliminary exploration of future too near, Asian J. Psychiatry 67 (2022), 102939.
[18] T. Wang, J. Liu, X. Luo, et al., Functional metabolomics innovates therapeutic discovery of traditional Chinese medicine derived functional compounds, Pharmacol. Ther. 224 (2021), 107824.
[19] Y. Chen, Q. Pu, F. Yu, et al., Comprehensive quantitative method for neurotransmitters to study the activity of a sedative-hypnotic candidate using microdialysis and LC × LC-MS/MS, Talanta 245 (2022), 123418.
[20] D. Shao, X. Liu, J. Wu, et al., Identification of the active compounds and functional mechanisms of Jinshui Huanxian formula in pulmonary fibrosis by integrating serum pharmacochemistry with network pharmacology, Phytomedicine 102 (2022), 154177.
[21] J. Wei, Y. Yu, Y. Zhang, et al., Integrated serum pharmacochemistry and network pharmacology approach to explore the effective components and potential mechanisms of menispermi rhizoma against myocardial ischemia, Front. Chem. 10 (2022), 869972.
[22] J.M. Moon, N. Thapliyal, K.K. Hussain, et al., Conducting polymer-based electrochemical biosensors for neurotransmitters: A review, Biosens. Bioelectron. 102 (2018) 540–552.
[23] R.I. Teleanu, A.G. Niculescu, E. Roza, et al., Neurotransmitters-key factors in neurological and neurodegenerative disorders of the central nervous system, Int. J. Mol. Sci. 23 (2022), 5954.
[24] J. He, C. Sun, T. Li, et al., A sensitive and wide coverage ambient mass spectrometry imaging method for functional metabolites based molecular histology, Adv. Sci. (Weinh.) 5 (2018), 1800250.
[25] X. Pang, S. Gao, M. Ga, et al., Mapping metabolic networks in the brain by ambient mass spectrometry imaging and metabolomics, Anal. Chem. 93 (2021) 6746–6754.
[26] D. Liu, J. Huang, S. Gao, et al., A temporo-spatial pharmacometabolomics method to characterize pharmacokinetics and pharmacodynamics in the brain microregions by using ambient mass spectrometry imaging, Acta Pharm. Sin. B 12 (2022) 3341–3353.
[27] B. Jin, X. Pang, Q. Zang, et al., Spatiotemporally resolved metabolomics and isotope tracing reveal CNS drug targets, Acta Pharm. Sin. B 13 (2023) 1699–1710.
[28] L. Chen, D. Xu, J. Kong, et al., Separation and identification of the hypnotic active ingredients of *Polygala tenuifolia* Willd, Food Mach 34 (2018) 119–122, 182.
[29] Y. Djeridane, B. Lemmer, Y. Touitou, Diazepam affects both level and amplitude of rat locomotor activity rhythm but has no effect on core body temperature, Chronobiol. Int. 22 (2005) 975–985.
[30] L. Lin, L. Yan, H. Zhang, et al., Simultaneous analysis of polygala acid, senegenin and 3,6'-disinapoylsucrose in rat plasma by liquid chromatography-tandem mass spectrometry: Application to a pharmacokinetic study after oral administration, Biomed. Chromatogr. 28 (2014) 594–600.
[31] X. Zhao, B. Xu, P. Wu, et al., UHPLC-MS/MS method for pharmacokinetic and bioavailability determination of five bioactive components in raw and various processed products of *Polygala tenuifolia* in rat plasma, Pharm. Biol. 58 (2020) 969–978.
[32] Z. Zhou, Y. Chen, J. He, et al., Systematic evaluation of serum and plasma collection on the endogenous metabolome, Bioanalysis 9 (2017) 239–250.
[33] X. Ren, G. Wang, X. Zhang, et al., Sedative and hypnotic effects and transcriptome analysis of *Polygala tenuifolia* in aged insomnia rats, Chin, J. Integr. Med. 26 (2020) 434–441.
[34] S.K. Wood, R.J. Valentino, The brain norepinephrine system, stress and cardiovascular vulnerability, Neurosci. Biobehav. Rev. 74 (2017) 393–400.
[35] A. Tavares, D.E. Handy, N.N. Bogdanova, et al., Localization of alpha 2A- and alpha 2B-adrenergic receptor subtypes in brain, Hypertension 27 (1996) 449–455.
[36] W. Peng, Z. Wu, K. Song, et al., Regulation of sleep homeostasis mediator adenosine by basal forebrain glutamatergic neurons, Science 369 (2020), eabb0556.
[37] T. Porkka-Heiskanen, L. Alanko, A. Kalinchuk, et al., Adenosine and sleep, Sleep Med, Rev. 6 (2002) 321–332.
[38] X. Dai, E. Zhou, W. Yang, et al., Molecular resolution of a behavioral paradox: Sleep and arousal are regulated by distinct acetylcholine receptors in different neuronal types in *Drosophila*, Sleep 44 (2021), zsab017.
[39] F. Weber, Y. Dan, Circuit-based interrogation of sleep control, Nature 538 (2016) 51–59.
[40] B. Platt, G. Riedel, The cholinergic system, EEG and sleep, Behav. Brain Res. 221 (2011) 499–504.
[41] M.M. Thakkar, Histamine in the regulation of wakefulness, Sleep Med, Rev. 15 (2011) 65–74.
[42] M. Shariatgorji, A. Nilsson, E. Fridjonsdottir, et al., Comprehensive mapping of neurotransmitter networks by MALDI-MS imaging, Nat. Methods 16 (2019) 1021–1028.
[43] R. Shariatgorji, A. Nilsson, E. Fridjonsdottir, et al., Spatial visualization of comprehensive brain neurotransmitter systems and neuroactive substances by selective *in situ* chemical derivatization mass spectrometry imaging, Nat. Protoc. 16 (2021) 3298–3321.
[44] Y.-H. Wu, D.F. Swaab, The human pineal gland and melatonin in aging and Alzheimer's disease, J. Pineal Res. 38 (2005) 145–152.
[45] A. Ni, C. Ernst, Evidence that substantia nigra pars compacta dopaminergic neurons are selectively vulnerable to oxidative stress because they are highly metabolically active, Front. Cell. Neurosci. 16 (2022), 826193.
[46] Y. Si, L. Wang, J. Lan, et al., Lilium davidii extract alleviates *p*-chlorophenylalanine-induced insomnia in rats through modification of the hypothalamic-related neurotransmitters, melatonin and homeostasis of the hypothalamic-pituitary-adrenal axis, Pharm. Biol. 58 (2020) 915–924.
[47] Y. Xu, L. Ma, F. Liu, et al., Lavender essential oil fractions alleviate sleep disorders induced by the combination of anxiety and caffeine in mice, J. Ethnopharmacol. 302 (2023), 115868.
[48] H. Xu, Z. Wang, L. Zhu, et al., Targeted neurotransmitters profiling identifies metabolic signatures in rat brain by LC-MS/MS: Application in insomnia, depression and Alzheimer's disease, Molecules 23 (2018), 2375.
[49] E. Costa, A. Guidotti, C.C. Mao, et al., New concepts on the mechanism of action of benzodiazepines, Life Sci 17 (1975) 167–185.
[50] G. Spadoni, A. Bedini, S. Rivara, et al., Melatonin receptor agonists: New options for insomnia and depression treatment, CNS Neurosci. Ther. 17 (2011) 733–741.
[51] A.D. Krystal, E. Richelson, T. Roth, Review of the histamine system and the clinical effects of H1 antagonists: Basis for a new model for understanding the effects of insomnia medications, Sleep Med, Rev. 17 (2013) 263–272.
[52] W.A. Santos Moraes, P.R. Burke, P.L. Coutinho, et al., Sedative antidepressants and insomnia, Braz. J. Psychiatry 33 (2011) 91–95.
[53] C. Gudex, Adverse effects of benzodiazepines, Soc. Sci. Med. 33 (1991) 587–596.
[54] K.Y. Shin, B.Y. Won, H.J. Ha, et al., Preclinical safety of the root extract of *Polygala tenuifolia* willdenow in sprague-dawley rats and beagle dogs, Evid. Based Complementary, Altern. Med. 2014 (2014), 570134.
[55] N.A. DeMartinis, A. Winokur, Effects of psychiatric medications on sleep and sleep disorders, CNS Neurol. Disord. Drug Targets 6 (2007) 17–29.
[56] A. Winokur, K.A. Gary, S. Rodner, et al., Depression, sleep physiology, and antidepressant drugs, Depress. Anxiety 14 (2001) 19–28.